Yukawa Institute Kyoto

YITP-98-68
October 1998

Microscopic Structure of Rotational Damping *

M. Matsuo[a], K. Yoshida[b], T. Døssing[c], E. Vigezzi[d], R.A. Broglia[c,d]

[a] *Yukawa Institute for Theoretical Physics, Kyoto University, Kyoto 606-8502, Japan*

[b] *Research Center for Nuclear Physics, Osaka University, Osaka 567-0047, Japan*

[c] *Niels Bohr Institute, University of Copenhagen, DK2100 Copenhagen Ø, Denmark*

[d] *INFN Sez. Milano, and Department of Physics, University of Milano, Milan 20133, Italy*

Abstract

The damping of collective rotational motion is studied microscopically, making use of shell model calculations based on the cranked Nilsson deformed mean-field and on residual two-body interactions, and focusing on the shape of the gamma-gamma correlation spectra and on its systematic behavior. It is shown that the spectral shape is directly related to the damping width of collective rotation, Γ_{rot}, and to the spreading width of many-particle many-hole configurations, Γ_{μ}. The rotational damping width is affected by the shell structure, and is very sensitive to the position of the Fermi surface, besides mass number, spin and deformation. This produces a rich variety of features in the rotational damping phenomena.

*A talk presented by M.M. at the *Topical Conference on Giant Resonances*, Varenna, May 11-16, 1998

1 Introduction

The collective rotation of deformed nuclei becomes a damped motion as the nuclei are thermally excited [1, 2, 3, 4]. It is known that the levels near the yrast line form rotational band structures based on simple configurations which are well described by cranked mean-field models. As the thermal excitation energy (i.e., the excitation energy measured from the yrast line) increases, the level density also increases steeply, so that the spacings between neighboring levels become smaller than the typical size ($\sim$ 10 keV) of the two-body matrix elements of the residual interaction. In such a situation, the pure configurations of the cranked mean-field get mixed and form compound states. Because of this configuration mixing, the rotational E2 decay from an off-yrast compound state (at spin I) may be fragmented over many final states (at $I-2$). The width of the associated strength function corresponds to the rotational damping width Γ_{rot}, that is, to the damping width of collective rotation.

A microscopic description of rotational damping is provided by a shell model diagonalization using the cranked Nilsson-Strutinsky mean-field and a two-body residual interaction such as the surface delta interaction (SDI) or the delta force [5, 6, 7]. It is important to include all many-particle many-hole (np-nh) configurations present in the energy region of interest in order to enable the shell model description of the off-yrast energy levels and of the associated rotational E2 transitions. This is possible since the intrinsic excitation energy which is relevant for the observed gamma-ray spectra is not very high (up to a few MeV), corresponding to about $10^2 - 10^3$ levels for each spin and parity in heavy nuclei, a number which can be handled by standard diagonalization techniques. Thus one can perform detailed studies of the microscopic structure of the damping of collective rotation. In this paper, we report our recent theoretical investigations, particularly concerning the spectral shape of damped rotational E2 transitions and its systematic behavior.

2 Rotational damping and doorway states of damped E2 transitions

Using the cranked shell model [2, 5, 7], the energy eigenstates (energy levels) at spin I are described as linear superpositions of basis cranked np-nh configurations $|\mu(I)\rangle$

$$|\alpha(I)\rangle = \sum_{\mu} X^{\alpha}_{\mu}(I)\,|\mu(I)\rangle \tag{1}$$

where the amplitude $X^{\alpha}_{\mu}(I)$ is determined by diagonalization of a shell model Hamiltonian and the basis space includes all np-nh configurations $|\mu(I)\rangle$ of the cranked Nilsson single-particle orbits. It is assumed that if the residual interaction were not present, the μ configurations would form rotational band structures, so that rotational E2 transitions would connect only states with the same configuration, with transition energy $E_{\gamma\mu} = E_{\mu}(I) - E_{\mu}(I-2) = 2\omega_{\mu}(I)$. The compound state $|\alpha(I)\rangle$, however, contains many

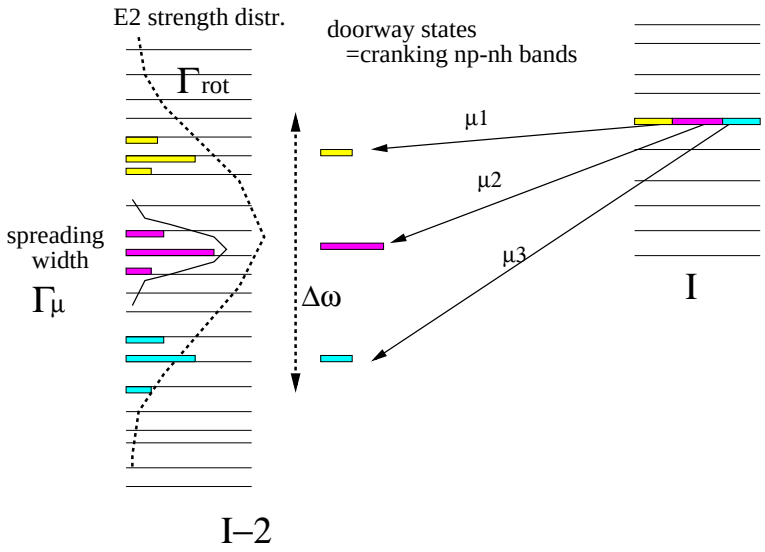

Figure 1: Schematic illustration of damped rotational E2 transitions in rotating nuclei. The horizontal bars represent the energy levels at spin I and $I-2$. The thick bars represent the strength of cranked shell model np-nh states. See also text.

μ states which in general have different transition energies $E_{\gamma\mu}$ (or different rotational frequency $\omega_\mu(I)$) because of the difference in the angular momentum alignments of nucleons occupying different orbits. The μ states at spin $I-2$ can then be regarded as doorway states for the damped rotational E2 decay from $\alpha(I)$. Since the doorway states are not energy eigenstates, they spread over compound states at $I-2$ (due to the residual two-body interaction) with spreading width Γ_μ. If the spreading width Γ_μ is small, the total E2 strength distribution reflects the distribution of doorway states, and its width, the rotational damping width Γ_{rot}, is proportional to the statistical dispersion $\Delta\omega$ of the rotational frequency ω_μ of cranked shell model np-nh states. In turn, the doorway structures are smeared by the the spreading width Γ_μ (See Fig.1), determining the fine structure of the strength distribution. If Γ_μ is larger than $\Delta\omega$ (the strong coupling limit), the doorway picture is lost, and one is in the region of the "motional narrowing" of the damping width. In this limit, the rotational damping width is estimated to be $\Gamma_{rot} \propto \Delta\omega^2/\Gamma_\mu$ [2].

For analyses of the rotational damping, it is useful to look at two coincident gamma-rays emitted in the E2 decay cascade [3, 4]. If there is no rotational damping, the rotational E2 transition takes place along the rotational bands, and the energy difference between two consecutive gamma's for $I+2 \rightarrow I$ and for $I \rightarrow I-2$ forms a sharp peak at $E_{\gamma 1} - E_{\gamma 2} = 4/\mathcal{J}$ because of the rotational correlation $E_\gamma \sim 2I/\mathcal{J} + \text{const.}$ ($\mathcal{J}$ being the rotational moment of inertia). For E2 transitions associated with the damped rotation, on the other hand, the gamma-gamma correlation spectrum shows a broadening around the same position, and the width of the correlation spectrum can then be related to the rotational damping width Γ_{rot} (Γ_{rot}=FHWM/2 by assuming a Gaussian distribution for the strength associated to a single transition step). The calculated spectra clearly show the change from the region of unperturbed rotational bands close to yrast, to the region of damped collective rotation, as a function of the intrinsic excitation energy U (see Fig.2 and

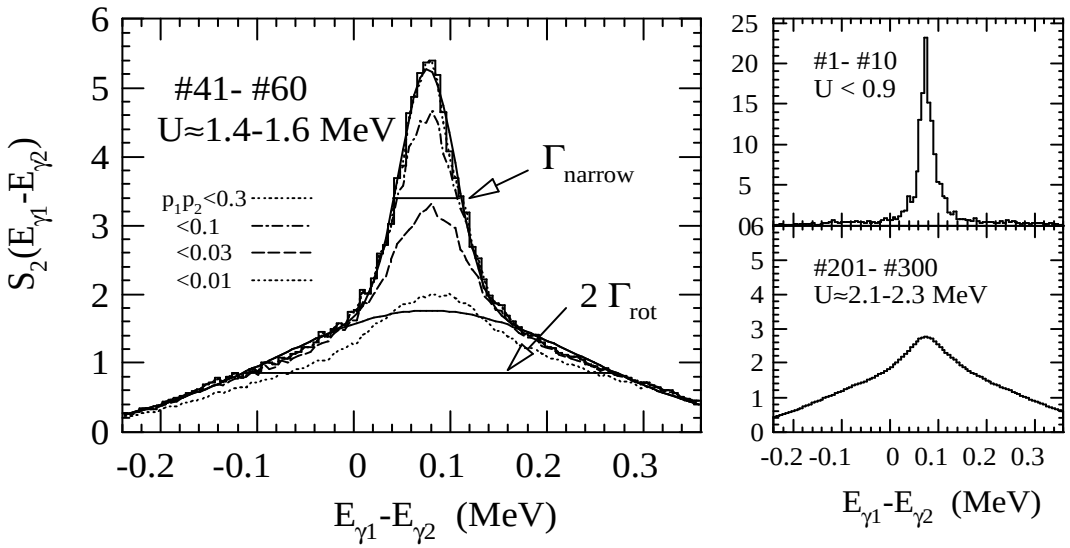

Figure 2: Calculated gamma-gamma correlation spectra for two consecutive E2 gamma rays $I+2 \rightarrow I$ ($E_{\gamma 1}$) and $I \rightarrow I-2$ ($E_{\gamma 2}$), projected on the axis $E_{\gamma 1} - E_{\gamma 2}$ for the levels of ^{168}Yb in the energy bins including the fist to 10th lowest levels (for each I^{π}), the 21-st to 40th, and the 250th to 300th covering different intrinsic excitation energy U in spin interval $I = 31 - 50$.

Ref.[7]). It should be noted, however, that the spectrum for the region of $U = 1-2$ MeV, which is most relevant to the experimental quasicontinuum gamma-ray spectra, shows neither the sharp peak associated with the band structure nor the broadened damped distribution. It has instead a more complex profile, which can be decomposed in the sum of two contributions, having wide and narrow distributions, as shown in Fig. 2 [7, 8].

3 The narrow component and spreading width of np-nh states

To understand the two-component profile, it is useful to reconsider the illustration of the rotational damping shown in Fig.1, where the E2 strength distribution is characterized not only by the damping width Γ_{rot} but also by the spreading width Γ_{μ} of the np-nh configurations. We can consider the same doorway states for feeding transitions from states at $I+2$ to the state α at I as those decaying from α at I to $I-2$. Taking the correlation between feeding and decaying transitions, the coincident transitions sharing the same doorway states (μ states) keep the rotational correlation up to the energy scale of Γ_{μ}, and their contribution form the narrow component of width $\sim \Gamma_{\mu}$ around $E_{\gamma 1} - E_{\gamma 2} = 4/\mathcal{J}$.

Indeed the calculations show a direct relation [9] between the spreading width Γ_{μ} and the width of the narrow component Γ_{narrow}. The latter can be extracted from the calculated gamma-gamma correlation spectra by a fit based on two gaussians (See Fig.2). On the other hand, the spreading width Γ_{μ} of the np-nh shell model configurations μ is defined

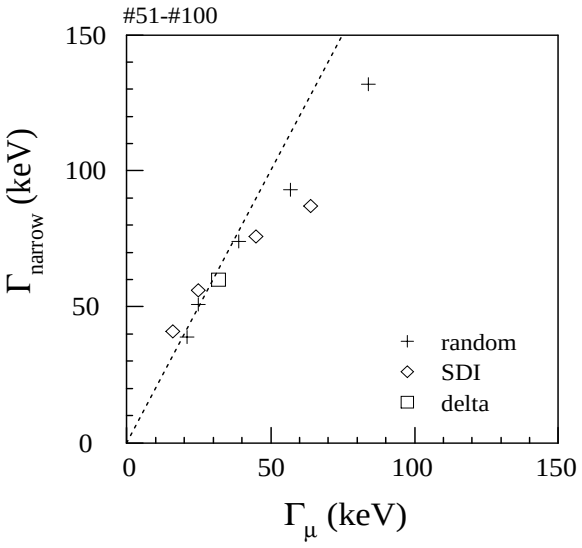

Figure 3: The width of the narrow component Γ_{narrow} of the gamma-gamma correlation spectra versus the spreading width Γ_μ of np-nh cranked shell model states, calculated for the energy bin including 51st to 100th levels (for each I^π) in the spin interval $I = 20 - 50$ in ^{168}Yb using three different residual two-body interactions (a random two-body int., the surface delta force, and the volume delta force) with various force strengths.

in terms of the strength function $S_\mu(E) = \sum_\alpha \left|X^\alpha_\mu\right|^2 \delta(E - E_\alpha)$ of the μ states which are embedded in the eigenstates α's[10]. The spreading width Γ_μ of μ states can be extracted by taking the autocorrelation of $S_\mu(E)$, then averaging over many μ states, and identifying a half of FWHM of the averaged autocorrelation function $C(e) = \langle \int dE S_\mu(E) S_\mu(E + e) \rangle$ as the spreading width Γ_μ. Figure 3 compares the extracted values of Γ_{narrow} and Γ_μ for different kinds and force strengths of the residual two-body interaction. There exists a clear and universal linear relation between the two widths.

4 Systematics and varieties of rotational damping

The microscopic calculations predict a large variation of rotational damping as a function of deformation, mass number and nuclear species. To demonstrate it, we show in Fig.4 the calculated gamma-gamma correlation spectra for several normal and superdeformed nuclei in different mass regions. Here ^{114}Te,^{168}Yb, and ^{234}U represent typical normal deformed nuclei in different mass regions. For ^{114}Te, quasicontinuum gamma-ray spectra from a fusion reaction suggest the presence of collective rotation in the high spin region $I \gtrsim 35\hbar$[11]. Rotational band structures were observed recently up to spin $I \sim 50\hbar$; the moment of inertia associated with the observed rotational bands decreases with spin, indicating that the collective rotation may terminate at the highest spins [12]. In the present calculation for ^{114}Te, we neglect the possibility of band termination and choose a fixed value for the deformation, for simplicity. ^{234}U is chosen as a typical deformed nucleus in the actinide region although it may not be very easy to feed very high spins because of the competition with fission. ^{143}Eu, ^{152}Dy, and ^{192}Hg are representative of superdeformed nuclei in $A \sim 150$ and 190 mass regions. For those nuclei, quasicontinuum E2 gamma-rays associated with superdeformed states are observed [13, 14, 15, 16]. The deformation parameters used in the calculation are $(\epsilon, \epsilon_4) = (0.25, 0.0), (0.255, 0.014), (0.226, -0.05)$ for ^{114}Te,^{168}Yb, ^{234}U respectively, and the same values as in Refs.[18, 19] for superdeformed ^{143}Eu, ^{152}Dy, and ^{192}Hg. For ^{114}Te, we used a modified Nilsson parameter[17]. As the

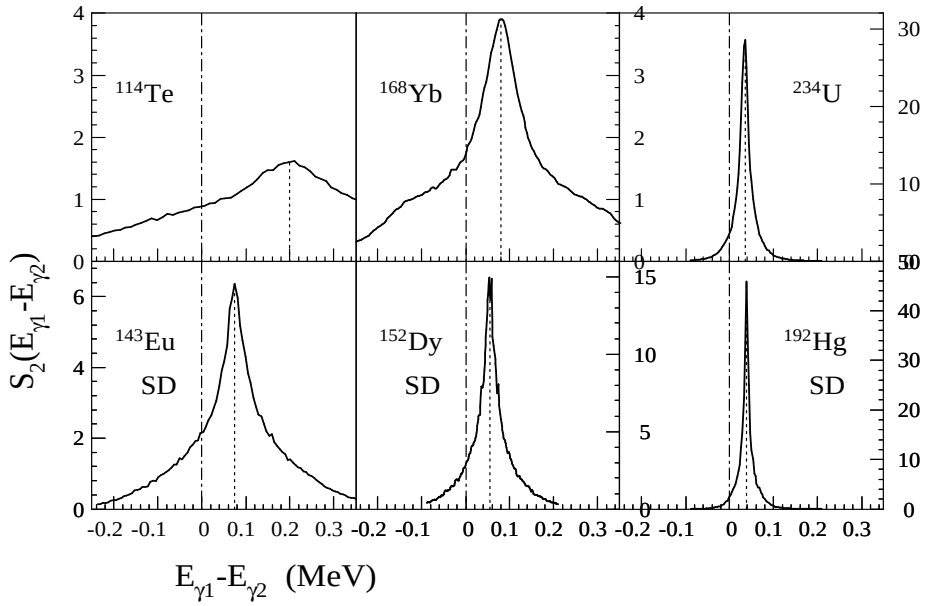

Figure 4: The gamma-gamma correlation spectra for normal deformed ^{114}Te, ^{168}Yb, ^{234}U, and superdeformed ^{143}Eu,^{152}Dy, ^{192}Hg. The spectrum is calculated for the states from 51st to 100th (for each I^π) in the spin region $I = 36-45$ ($I = 46-55$ for superdeformed ^{152}Dy and ^{143}Eu).

residual interaction, the surface delta interaction and the volume delta force with standard parameters [7] are used for normal and superdeformed nuclei, respectively. See Refs.[7, 18, 19] for further details.

The results shown in Fig. 4 present significantly different gamma-gamma correlation spectra in different nuclei. Qualitatively, the width of the spectrum decreases with increasing mass number and deformation, in agreement with an analytic estimate by Lauritzen et al. [2]. The rotational damping width extracted from the gamma-gamma correlation spectra by the method of the two gaussian fit (See Fig.2) is summarized in Table 1. The damping width in SD ^{192}Hg is as small as 20 keV, that is, almost 10 times smaller than in the typical rare-earth normal deformed nucleus ^{168}Yb.

The systematic behavior can be understood microscopically. The rotational damping width Γ_{rot} is dominated by the dispersion of rotational frequency $\Delta\omega$ as illustrated in

Table 1: The calculated rotational damping width Γ_{rot} and the spreading width Γ_μ cranked shell model np-nh states for ^{114}Te, ^{168}Yb, ^{234}U, ^{143}Eu, ^{152}Dy and ^{192}Hg. The same energy bin and spin interval as in Fig.4 are considered.

	^{114}Te	^{168}Yb	^{234}U	^{143}Eu(SD)	^{152}Dy(SD)	^{192}Hg(SD)
Γ_{rot} (keV)	387	224	33	143	67	23
Γ_μ (keV)	98	45	46	43	59	28

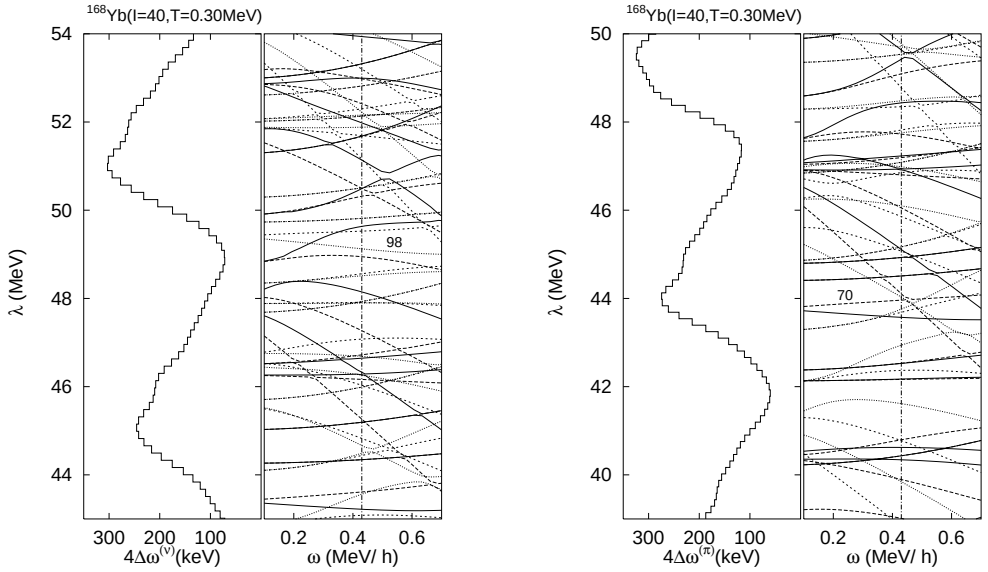

Figure 5: The cranked Nilsson single-particle levels as a function of rotational frequency ω for ^{168}Yb for neutrons (left panel) and protons (right panel), are plotted in the right part of each panel. In the left part of each panel, the neutron and proton contribution to the dispersion of rotational frequency $\Delta\omega$ is plotted as a function of the Fermi energy λ for $\omega = 0.434$ MeV and $T = 0.3$ MeV, corresponding to $I = 40, U \sim 2$ MeV

Fig.1. The dispersion $\Delta\omega$ arises from the particle alignments along the rotational axis. The alignments are different depending on the cranked single-particle orbits; some are highly alignable (steeply down-sloping as ω increases), while some show small alignments as shown in Fig. 5. The highly aligned orbits are intruder orbits with high-N and low-Ω, and therefore they are located in a specific region in a shell of the cranked single-particle spectrum. This shell structure causes the dispersion $\Delta\omega$ of rotational frequency to oscillate strongly as a function of the position of the Fermi surface, in addition to the background smooth dependence [2] $\Delta\omega \propto IA^{-5/2}\epsilon^{-1}$ on spin I, quadrupole deformation ϵ, and the mass number A. Figure 5 also plots the value of $\Delta\omega$ as a function of the Fermi energy λ, evaluated microscopically as $\Delta\omega = \frac{1}{\mathcal{J}}\sqrt{\sum_n i_n^2 f_n(1-f_n)}$ [20] using the single-particle alignments i_n and the Fermi-Dirac thermal distribution $f_n = (1+\exp\frac{e_n-\lambda}{T})^{-1}$. One clearly sees a shell oscillation pattern with a large amplitude: maximum and minimum differ by more than a factor 2. It is noted that the difference in the rotational damping width Γ_{rot} between SD ^{143}Eu and SD ^{152}Dy is considerable in spite of the small difference in deformation and mass number. This arises from the shell structure of the single-particle alignments, which is also responsible for the extremely small value of Γ_{rot} in SD ^{192}Hg [19].

The extracted spreading width Γ_μ of np-nh cranked shell model states is also listed in Table 1 together with Γ_{rot}. Compared with the large variation in Γ_{rot}, the spreading width takes more or less similar value for different mass regions. It is noted that Γ_{rot} is larger than the spreading width Γ_μ in ^{168}Yb, which implies the weak coupling situation

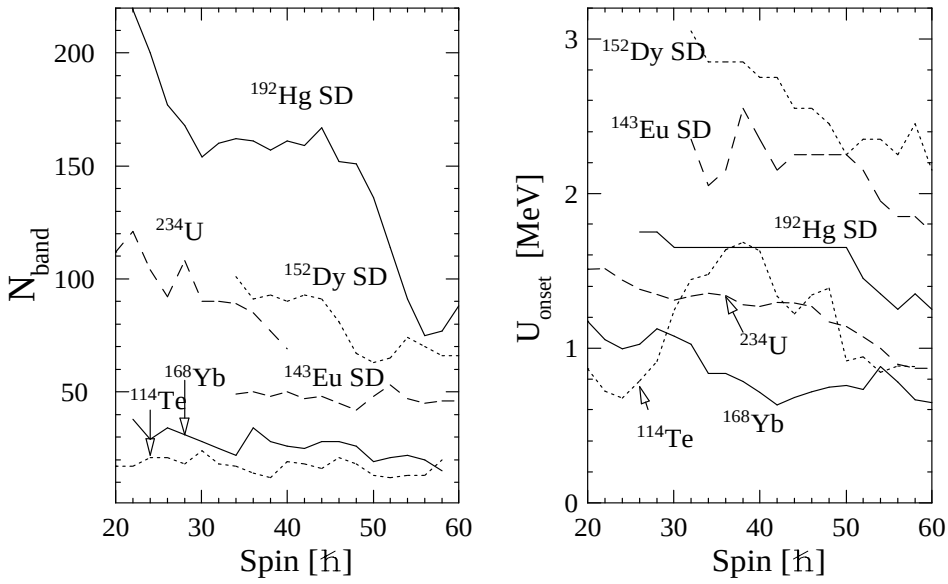

Figure 6: The number of rotational bands N_{band} and the onset energy U_{onset} of rotational damping for normal deformed^{114}Te, ^{168}Yb, ^{234}U and superdeformed ^{143}Eu,^{152}Dy, ^{192}Hg, as a function of spin.

for which the concept of doorway states is meaningful. Accordingly the gamma-gamma correlation spectrum displays the two-component profile. The weak coupling situation holds also for ^{114}Te and SD ^{143}Eu. On the contrary, the spreading width Γ_μ is comparable with or slightly smaller than Γ_{rot} for superdeformed ^{192}Hg, ^{152}Dy, and normal deformed ^{234}U. If $\Gamma_\mu \ll \Gamma_{rot}$ held, the "motional narrowing" would be expected. SD ^{192}Hg, SD ^{152}Dy, and ^{234}U are situated at the borderline for onset of the motional narrowing.

A variety of features is also seen considering the onset of the rotational damping. Figure 6 shows the excitation energy U_{onset}(measured from the yrast line) where the damping sets in, and the number N_{band} of rotational bands which lie near the yrast line, surviving against the rotational damping [7, 18, 19]. Compared to the typical example ^{168}Yb of rare-earth normal deformed nuclei, the onset energy is higher in superdeformed ^{143}Eu and ^{152}Dy by more than 1 MeV. This is because the level density of superdeformed states is much lower than in normal deformed nuclei due to the shell gap in the cranked single-particle spectrum[5, 18]. Also the value of N_{band} is larger than in ^{168}Yb. It is noted that N_{band} for superdeformed ^{192}Hg reaches 150. In SD ^{192}Hg the level density is not as small as in other SD nuclei, and the anomalously large value of N_{band} is not explained by the level density effect. Instead, this is caused by the extremely small rotational damping width $\Gamma_{rot}\sim$ 20 keV, which is comparable with the level spacing ($d = 30 - 10$ keV) in the onset region ($E = 1.2 - 1.6$ MeV)[19]. If $\Gamma_{rot} \ll d$, the configuration mixing among np-nh cranked shell model states should not lead to the damping of rotation, as was discussed by Mottelson [21]; one should instead expect rotational band structures built upon the strongly mixed compound states, the so called "ergodic rotational bands" [22]. The case of SD ^{192}Hg is close to the borderline for the emergence of such ergodic rotational bands [19].

References

[1] G.A. Leander, Phys. Rev. C25(1982)2780.

[2] B. Lauritzen, T. Døssing, and R.A. Broglia, Nucl. Phys. A457(1986)61.

[3] B. Herskind, et al., Phys. Rev. Lett. 68(1992)3008;
T. Døssing, et al., Phys. Rep. 268(1996)1.

[4] B. Herskind, et al., Phys. Lett. B276(1992)4.

[5] S. Åberg, Phys. Rev. Lett. 64(1990)3119;
S. Åberg, Prog. Part. Nucl. Phys. vol.28 (Pergamon 1992) p.11.

[6] M. Matsuo, T. Døssing, E. Vigezzi and R.A. Broglia, Phys. Rev. Lett. 70(1993)2694.

[7] M. Matsuo, T. Døssing, E. Vigezzi, R.A. Broglia, and K. Yoshida, Nucl. Phys. A617(1997)1.

[8] R.A. Broglia, et al., Z. Phys. A356(1996)259.

[9] M. Matsuo, T. Døssing, E. Vigezzi and R.A. Broglia, in preparation.

[10] A. Bohr and B.R. Mottelson, *Nuclear Structure.* vol. I (Benjamin, 1969).

[11] M.A. Deleplanque, et al., Phys. Rev. Lett. 40(1978)629; *ibid.* 41(1978)1105.

[12] I. Thorslund, et al., Phys. Rev. C52(1995)R2839.

[13] S. Leoni, et al., Phys. Rev. Lett. 76(1996)3281.

[14] K. Schiffer and B. Herskind, Phys. Lett. B255(1991)508

[15] T. Lauritsen, et al., Phys. Rev. Lett. 69(1992)2479.

[16] R.G. Henry, et al., Phys. Rev. Lett. 73(1994)777.

[17] Jing-ye Zhang, et al., Phys. Rev. C39(1989)714.

[18] K. Yoshida and M. Matsuo, Nucl. Phys. A612(1997)26.

[19] K. Yoshida and M. Matsuo, Nucl. Phys. A636(1998)169.

[20] T. Døssing and B. Herskind, Proc. Intern. Symp. on New Trends in Nuclear Collective Dynamics (Nishinomiya) (Springer-Verlag, 1992) p.239.

[21] B.R. Mottelson, Nucl. Phys. A557(1993)717c.

[22] S. Åberg, Z. Phys. A358(1997)269